between $\pm{}^1/_2$ and $\pm{}^3/_2$ ground-state levels on the basis of observed g' values. For the $\pm{}^3/_2$ state the spectra are practically axial in that case, with $g_\perp = 0$–1 and $g_\parallel = 6$–7. For small λ values and $\pm{}^3/_2$ state, an EPR spectrum can be difficult to detect, since the spectrum would consist of a very small absorption below 100 mT at X-band and a perpendicular peak at very high magnetic field. This situation has been found in bis(*N-tert*-butylpyrrolecarbaldimino)cobalt(II), which at X-band does not show any EPR signal at all.[13] For λ values close to the critical value of $\lambda = {}^1/_3$, it is practically impossible to distinguish between $\pm{}^1/_2$ and $\pm{}^3/_2$ states, since in both cases a nearly axial spectrum with $g'_\parallel > g'_\perp$ is expected. The general picture of $g'(\lambda)$ discussed above for Co(II) tetrahedral complexes can be influenced by two factors. Equations 2 are the first approximation of a more general expression, and contributions from higher order terms can be expected,[11] especially in the case of $|2D| < 3$ cm^{-1}. In a low crystal field symmetry a noncollinearity of the $\mathbf{g}^2$ tensor and $\mathbf{D}$ tensor can appear[10] and lead to large variations of apparent g' values, even in the case of a small value of rhombic parameter E.

Acknowledgment. This work was partly carried out under the Project MR I.9.

Registry No. cin(CoCl$_4$), 97150-36-2.

Contribution from the Department of Chemistry and Biochemistry,
University of California at Los Angeles, Los Angeles, California 90024

Calculation of the Electronic Spectra of Conjugated Cyclic PNS Ring Systems from Preresonance Raman Fundamental and Overtone Intensities

YUN-YEN YANG and JEFFREY I. ZINK*

Received October 26, 1984

Low-temperature electronic absorption spectra and preresonance Raman spectra of Ph$_2$PS$_2$N$_3$ (I) and Ph$_4$P$_2$S$_2$N$_4$ (II) are obtained. The absorption spectrum of I exhibits vibronic structure. An overtone in the Raman spectrum of II shows significant intensity. Excited-state distortions of the two compounds are calculated by using the time-dependent theory of electronic and Raman spectroscopy. The electronic absorption spectra are calculated from the Raman-determined data. An excited-state distortion is independently calculated from the overtone intensity in the Raman spectrum. In all cases excellent agreement between experiment and theory is obtained. The distortions of I are compared to those expected from molecular orbital theory.

The time-dependent theory of molecular spectroscopy provides a powerful method for determining excited-state distortions and understanding the details of electronic spectra.[1] It provides both intuitive and quantitative understanding of the connections between preresonance Raman spectroscopy, electronic absorption and emission spectroscopy, and geometry changes between the ground and excited electronic states. The theory has been applied to a limited number of transition-metal,[2,3] organometallic,[4,5] and organic systems.[6]

During the course of our studies of the quantitative relationship between preresonance Raman spectroscopy and electronic spectroscopy, our interest was aroused by the delocalized π systems in inorganic ring compounds. The compounds 5,5-diphenyl-$1\lambda^4,3\lambda^4,2,4,6,5\lambda^5$-dithiatriazaphosphorine (I) and 5,5,7,7-tetraphenyl-$1\lambda^4,3\lambda^4,2,4,6,8,5\lambda^5,7\lambda^5$-dithiatetrazadiphosphocine (II) proved especially useful for study.[7,8] Both compounds have intense electronic transitions in the visible region of the spectrum. As reported below, I exhibits resolved vibronic structure at low temperature and II has significant overtone intensity from a normal mode in its Raman spectrum. These compounds thus provide a test of the applicability of the theory to a previously unstudied type of molecule and electronic transition. In addition, the results provide insight into the electronic structure of this interesting class of molecules. We report here the low-temperature single-crystal electronic absorption spectra, the preresonance Raman spectra, and the quantitative interrelationship between the two in terms of displacements of the excited electronic state along normal coordinates.

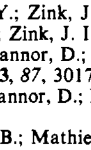

I

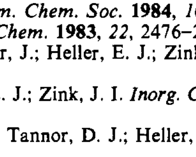

II

Experimental Section

Samples were donated by Prof. Chivers. The techniques for obtaining the low-temperature absorption spectra were described elsewhere.[9] The Raman spectra were recorded by using an RCA C31034-02 phototube, a PAR Model 1105 photon counter, and a Spex 1401 monochromator. Excitation radiation was provided by a Spectra Physics argon ion laser and a krypton ion laser. The monochrometer and photon counter were controlled by a PDP 11/02 computer. The Raman spectra were collected and stored digitally.

Theory

The time-dependent theory of molecular spectroscopy provides both a quantitative and an intuitive physical picture of the interrelationship between preresonance Raman spectra and electronic absorption spectra.[1] In both types of spectroscopy, the spectra are governed by the motion of a wave packet on a multidimensional excited-electronic-state potential hypersurface. A cross section of the multidimensional surface along one normal mode, which will be used to discuss the theory, is shown in Figure 1.

The absorption process according to time-dependent theory[10] is illustrated on the left side of Figure 1. The initial vibrational wave packet, ϕ, propagates on the upper potential surface, which, in general, is displaced relative to the ground surface. The displaced wave packet is not a stationary state and evolves according

---

(1) Heller, E. J. *Acc. Chem. Res.* **1981**, *14*, 368–375.
(2) Yang, Y. Y.; Zink, J. I. *J. Am. Chem. Soc.* **1984**, *106*, 1500–1501.
(3) Yoo, C. S.; Zink, J. I. *Inorg. Chem.* **1983**, *22*, 2476–2477.
(4) Tutt, L.; Tannor, D.; Schindler, J.; Heller, E. J.; Zink, J. I. *J. Phys. Chem.* **1983**, *87*, 3017–3018.
(5) Tutt, L.; Tannor, D.; Heller, E. J.; Zink, J. I. *Inorg. Chem.* **1982**, *21*, 3859.
(6) Myers, A. B.; Mathies, R. A.; Tannor, D. J.; Heller, E. J. *J. Chem. Phys.* **1982**, *77*, 3857–3866.
(7) Burford, N.; Chivers, T.; Cordes, A. W.; Laidlaw, W. G.; Noble, M. C.; Oakley, R. T.; Swepton, P. N. *J. Am. Chem. Soc.* **1982**, *104*, 1282–1290.
(8) Burford, N.; Chivers, T.; Richardson, J. F. Inorg. *Chem.* **1983**, *22*, 1482–1487.
(9) Chang, T. H.; Zink, J. I. *J. Am. Chem. Soc.* **1984**, *106*, 287.
(10) Heller, E. J. *J. Chem. Phys.* **1978**, *68*, 3891–3896.

0020-1669/85/1324-4012$01.50/0

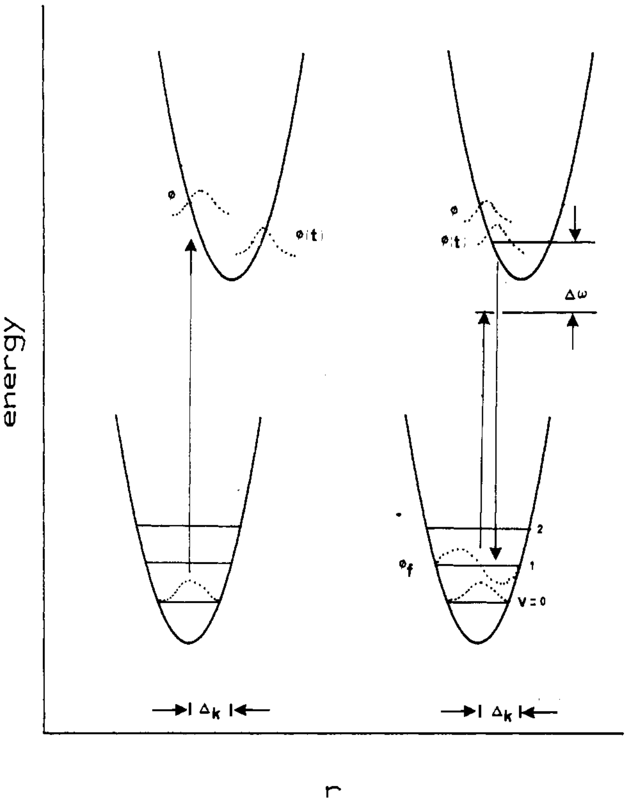

Figure 1. Illustrations of the time-dependent theory of electronic absorption (left) and Raman scattering (right).

to the time-dependent Schrödinger equation. The quantity of interest is the overlap of the initial wave packet with the time-dependent wave packet $\langle\phi|\phi(t)\rangle$. The overlap is a maximum at $t = 0$ and decreases as the wave packet moves away from its initial position. At some later time t, the wave packet may return to its initial position, giving rise to a recurrence of the overlap. A plot of the overlap as a function of time in the time domain shows the initial overlap decreasing and then recurring at a time t when the wave packet (and thus all of the atoms in the molecule) returns to its original position. This pattern is repetitive. In the simple case of harmonic potential surfaces and no change in vibrational frequencies between the ground and excited electronic states, the overlap is

$$\langle\phi|\phi(t)\rangle = \exp[-\sum_k[(\Delta_k^2/2)(1 - \exp(-i\omega_k t)) - i\omega_k t/2] - iE_0 t/h - \Gamma^2 t^2] \quad (1)$$

where E_0 is the energy difference between the minima of the two surfaces, Γ is a phenomenological damping factor (vide infra), and ω_k and Δ_k are the frequency and the displacement of the kth normal mode.[11]

The electronic absorption spectrum in the frequency domain is the Fourier transform of the overlap in the time domain. The absorption spectrum is then given by

$$I(\omega) = C\omega\int_{-\infty}^{\infty} e^{i\omega t}\langle\phi|\phi(t)\rangle\, dt \quad (2)$$

where C is a constant, ω is the frequency of incident radiation, and the other quantities are those defined above. Thus, the absorption spectrum can be calculated when the frequencies ω_k and the displacements Δ_k of the normal modes are known.

The time-dependent picture of Raman spectroscopy[12] is shown on the right side of Figure 1. Again the initial wave packet propagates on the upper excited-electronic-state potential surface. However, the quantity of interest is the overlap of the time-dependent wave packet with the *final* state ϕ_f, i.e. $\langle\phi_f|\phi(t)\rangle$. The Raman scattering amplitude in the frequency domain is the half Fourier transform of the overlap in the frequency domain

$$\alpha_{fi}(\omega_I) = \int_0^{\infty} e^{i\omega_I t - \Gamma t}\langle\phi_f|\phi(t)\rangle\, dt + (\mathrm{NRT}) \quad (3)$$

The point of connection between the apparently disparate electronic and Raman spectroscopies can be readily seen: in both cases the time-dependent wave packet is moving on the same excited-state potential surface.

It is very difficult to obtain experimentally the values of the scattering cross section. However, it is relatively easy to obtain the intensity of given normal mode k relative to that of another mode k'. A simple expression relating the relative intensities has been derived for the special conditions of harmonic oscillators, no Duschinsky rotation, no change in normal mode frequencies, and preresonance (short time) condition spectra. Under these conditions the relative intensities of two modes is given by[12,13]

$$\frac{I_k}{I_{k'}} = \frac{\Delta_k^2\omega_k^2}{\Delta_{k'}^2\omega_{k'}^2} \quad (4)$$

The important experimental condition that must be fulfilled is the short time, preresonance condition.[12] When the incident frequency is slightly off resonance with the excited electronic state of interest, the propagation time of the wave packet on the upper potential surface is governed by the time–energy uncertainty principle, $\Delta\omega\Delta t \cong 1$, where $\Delta\omega$ is the frequency mismatch. Under short time conditions the wave packet moves in a region localized near the equilibrium geometry of the ground electronic state, i.e. the Franck–Condon region. The preresonance Raman intensity is dominated by the slope of the potential surface in this region. The greater the slope, the greater the motion of the wave packet in Figure 1, the greater the overlap with the final state, and the greater the intensity.

The intensities of the first overtones in a preresonance Raman spectrum are determined by the overlap $\langle\phi_2|\phi_0(t)\rangle$ where ϕ_0 is the ground-vibration-state wave packet and ϕ_2 is the first overtone in a given mode.[2] Two limiting mechanisms have been derived from time-dependent theory to explain nonzero overlap and thus overtone intensity: displaced excited states and vibrational frequency changes in excited states. When the excited state is displaced relative to the ground state, the ratio of the intensity of the overtone to the fundamental for a given mode k is given by

$$\frac{I_{20}^k}{I_{10}^k} = \frac{(V_k)^2}{4\omega_k\sigma^2}\,\frac{\epsilon_2\left(\dfrac{\omega_e - E}{\sigma}\right)}{\epsilon_1\left(\dfrac{\omega_e - E}{\sigma}\right)} \quad (5)$$

where V_k is the first derivative of the upper potential surface at the ground-state equilibrium geometry, σ is related to the absorption bandwidth, and ϵ is a function based on the energy difference between the absorption band maximum E and the laser Raman excitation ω_e. When vibrational frequency changes govern the overtone intensity, the ratio of the overtone to the fundamental intensity is given by

$$\frac{I_{20}^k}{I_{10}^k} = \frac{(\omega_k^2 - V_{kk})^2}{4\omega_k V_k^2} \quad (6)$$

where V_{kk} is the second derivatve of the upper potential surface at the ground-state equilibrium geometry and the other symbols have been defined previously. The displaced excited-state

---

(11) In all of the calculations in this paper we use dimensionless normal coordinates. See ref 4 for details.

(12) Heller, E. J.; Sundberg, R. L.; Tannor, D. *J. Phys. Chem.* **1982**, *86*, 1822–1833.

(13) Equation 4 is a special case of the Savin formula: Tang, J.; Albrecht, A. C. In "Raman Spectroscopy"; H. Szynanski, Ed.; Plenum Press: New York, 1970; Vol. 2, p 33. Savin, F. A. *Opt. Spektrosk.* **1965**, *19*, 555. Warshel, A.; Dauber, P. *J. Chem. Phys.* **1977**, *66*, 5477. Clark, R.; Dines, P. *Mol. Phys.* **1981**, *42*, 193.

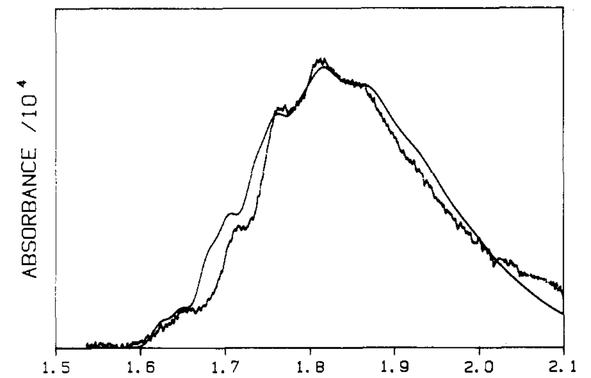

Figure 2. Experimental absorption spectrum of the HOMO → LUMO transition of $Ph_2PS_2N_3$ (dotted) and the calculated spectrum (solid). The calculated spectrum used $\Gamma = 76$, $E_0 = 16\,250$ cm^{-1}, and the following frequencies (cm^{-1}) and displacements (dimensionless normal coordinates): 242, 1.7; 505, 0.82; 570, 2.0; 700, 1.3.

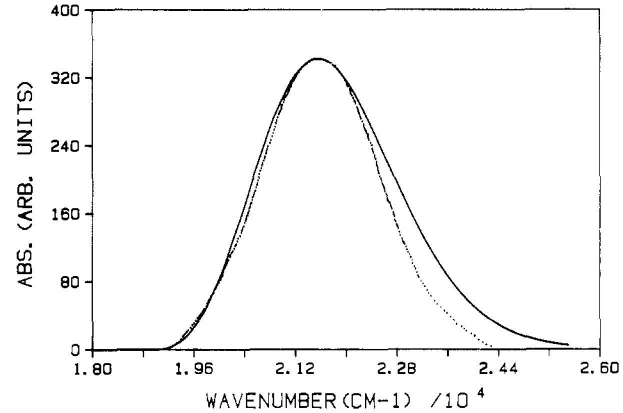

Figure 3. Experimental absorption spectrum of the HOMO → LUMO transition of $Ph_4P_2S_2N_4$ (dotted) and the calculated spectrum (solid). The calculated spectrum used $\Gamma = 92$, $E_0 = 19\,400$ cm^{-1} and the following frequencies (cm^{-1}) and displacements (dimensionless normal coordinates): 237, 1.6; 252, 1.5; 279, 1.0; 307, 0.80; 370, 0.80; 500, 0.4; 528, 0.6; 566, 1.10; 602, 0.60; 669, 1.6; 3068, 0.04; 3086, 0.04.

mechanism is expected to be the most important as resonance is approached, an expectation that can be experimentally tested. When the potential surfaces are harmonic, eq 5 can be rewritten in the form

$$\Delta_k^2 = \frac{I_{20}^k}{I_{10}^k}\,\frac{4\sigma^2}{\omega_k^2}\,\frac{\epsilon_1\left(\dfrac{\omega_e - E}{\sigma}\right)}{\epsilon_2\left(\dfrac{\omega_e - E}{\sigma}\right)} \qquad (7)$$

The displacement calculated from the overtone intensity by using eq 7 provides a useful cross-check on the displacements calculated from the fundamental intensities by using eq 4.

Spectra

The 10 K electronic absorption spectra in the visible region of the six- and eight-membered ring systems I and II are shown in Figures 2 and 3, respectively. The spectrum of I shows a clearly apparent vibronic structure at 10 K, which was not evident in the room-temperature spectrum. The peak maximum at 18 185 cm^{-1} in the low-temperature spectrum agrees very well with that reported at 18 180 cm^{-1} in dichloromethane solution at room temperature.[7]

The vibronic structure in the spectrum of I is not regularly spaced. The individual peaks are observed at 16 547, 17 122, 17 682, 18 185, and 18 674 cm^{-1}. The vibronic spacings are 575, 560, 503, and 489 cm^{-1}. The observed structure does not arise from a single progression in a single normal mode, but instead is a result of four highly displaced normal modes (vide infra).

Table I. Raman Intensities and Calculated Distortions of $Ph_2PS_2N_3$

ω_k, cm^{-1}	I_k/I_{623}[a]	Δ_k[b]
242	0.11 ± 0.02	1.7
505	0.11 ± 0.02	0.82
623	1.00	2.00
700	0.83 ± 0.17	1.3

[a] Integrated intensity ratios from 647.1-nm excitation. [b] Calculated displacements of dimensionless normal coordinates.

Table II. Raman Intensities and Calculated Distortions of $Ph_4P_2S_2N_4$

ω_k, cm^{-1}	I_k/I_{669}[a]	Δ_{exptl}[b]	Δ_{calcd}[c]
237	0.110 ± 0.011	1.50 ± 0.30	1.6
252	0.114 ± 0.011	1.44 ± 0.29	1.6
279	0.0566 ± 0.0057	0.91 ± 0.18	1.0
307	0.0817 ± 0.0082	0.62 ± 0.13	0.80
370	0.0561 ± 0.0056	0.69 ± 0.14	0.80
500	0.0342 ± 0.0034	0.40 ± 0.08	0.40
528	0.0877 ± 0.0088	0.61 ± 0.13	0.60
566	0.364 ± 0.036	1.14 ± 0.22	1.10
602	0.151 ± 0.015	0.69 ± 0.14	0.60
669	1.0	1.6	1.6
3068	0.0576 ± 0.0058	0.083 ± 0.034	0.04
3086	0.0566 ± 0.0057	0.083 ± 0.034	0.04
1342[d]	0.24 ± 0.04	1.5 ± 0.3[e]	

[a] Integrated intensity ratios from 514.5-nm excitation. [b] Distortions in dimensionless normal coordinates calculated by using eq 4. [c] Distortions used to calculate the electronic spectrum shown in Figure 3. [d] First overtone of the 669-cm^{-1} fundamental. [e] Displacement calculated from eq 7.

The 18 185-cm^{-1} band in compound I has been assigned to a $\pi^* \rightarrow \pi^*$ HOMO to LUMO transition. Chivers, Laidlow, Oakley, et al. have carried out a detailed molecular orbital analysis of the bonding and electronic structure of this compound.[7] A starting point for interpreting the electronic spectrum is to consider the compound to be an eight-electron, six-member ring delocalized π system. This simple picture then permits comparison with benzene or $S_3N_3^-$ (the latter being a D_{3h} ten-electron six-membered ring delocalized π system.) The doubly degenerate π-antibonding orbitals in the latter two compounds are split into two nondegenerate π-antibonding orbitals in the lower symmetry $H_2PS_2N_3$ compound. The HOMO is the lower component of this π-antibonding pair while the LUMO is the higher component. In addition to the HOMO to LUMO transition in the visible region of the spectrum, other absorption bands corresponding to transitions from the other occupied orbitals of π symmetry to the LUMO are observed in the UV region of the spectrum.

The 10 K electronic absorption spectrum of the eight-membered ring compound II is shown in Figure 3. An unstructured peak centered at 21 500 cm^{-1} is observed. This position of this peak is almost unchanged from the 21 505-cm^{-1} peak observed at room temperature in solution.[8]

The preresonance Raman spectrum of compound I was obtained by using the 6471-Å line from a krypton ion laser. Four intense bands were observed in the spectrum. The frequencies and the integrated intensities of these bands are given in Table I. The preresonance Raman spectrum of compound II was obtained by using the 514.5-nm argon ion laser line. Thirteen intense bands were observed in the spectrum. The frequencies and integrated intensities are listed in Table II. The appearance of an intense overtone band at 1342 cm^{-1} is of importance to the following calculations. Its intensity is one-fourth that of the intensity of the fundamental at 669 cm^{-1}. The overtone band was not observed in the "normal Raman" spectrum excited by the HeNe laser line at 632.8 nm.

Discussion

$Ph_2PS_2N_3$ (I). The electronic absorption spectrum of compound I is calculated by using the time-dependent theory of electronic spectroscopy. In order to calculate the spectrum, which is the Fourier transform of the time-dependent overlap in eq 1, the

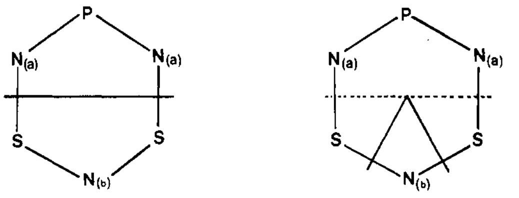

HOMO (2A$_2$) LUMO (4B$_1$)

Figure 4. Nodal planes of the ground electronic state (left) and excited electronic state (right) of I. The solid line indicates strong antibonding and the dashed line weaker antibonding. The positions of the nodes shown here were taken from the overlap populations calculated in ref 7.

frequencies and the displacements of the normal modes that contribute are required. These frequencies and displacements are independently determined from the preresonance Raman spectrum and eq 4. The data are given in Table I. The electronic spectrum calculated by using *exactly* the Raman-determined displacements is shown in Figure 2. A very good fit to the observed electronic spectrum is obtained. The irregularly spaced vibronic peaks result from contributions from all four of the highly displaced normal modes. The small deviations in intensity between the calculated and observed spectra are probably the result of anharmonicities and frequency changes in the excited state, which were not included in the calculation.

The calculated excited-state distortions are correlated with the excited-state bonding changes, which can be determined from the molecular orbital calculations of Chivers, Laidlaw, et al.[7] Representations of the nodal structures of the HOMO and the LUMO are shown in Figure 4. According to the calculated overlap populations, the HOMO is bonding between the phosphorus and nitrogen, nonbonding between sulfur and nitrogen(b), and antibonding between sulfur and nitrogen(a). The LUMO is antibonding between the sulfur and both types of nitrogen with the largest antibonding between sulfur and nitrogen(b). Thus the largest bonding change caused by the HOMO to LUMO transition is expected to be between sulfur and nitrogen(b). The smallest change is between phosphorus and nitrogen. A tentative assignment of the 623-cm^{-1} normal mode to a stretch primarily S–N$_b$ in character provides a consistent relationship between the distortions calculated from time-dependent theory and the bonding changes determined from the molecular orbital calculation.

$Ph_4P_2S_2N_4$ (II). The electronic spectrum of the eight-membered ring system II does not contain as much information as that of the six-membered ring system because of the lack of vibronic structure. The absence of vibronic structure is understandable in terms of the preresonance Raman data, which show that a much larger number of normal modes are highly displaced in the former compound. The broad envelope has been filled in by the vibrational modes. The electronic spectrum calculated from the Raman-determined displacements and frequencies is shown in Figure 3. An excellent fit is obtained on the low-energy side of the experimental spectrum. The small deviation on the high-energy side probably results from the neglect of anharmonicities and vibrational frequency changes in the excited state.

The most highly distorted normal mode is the 669-cm^{-1} mode. Although assignments of the vibrational spectrum have not been made, this mode can be tentatively assigned to a vibration primarily sulfur–nitrogen stretch in character. The overtone of this mode has significant intensity in the preresonance Raman spectrum (vide infra). Other highly displaced modes are probably stretching and torsional modes in the eight-membered ring. The high frequency modes above 3000 cm^{-1}, which are probably primarily C–H stretching vibrations, have very small but nonzero displacements.

A critical test of the time-dependent theoretical calculation of the displacement of the 669-cm^{-1} normal mode is provided by the overtone of this mode in the Raman spectrum. The displacement can be calculated by using eq 6, thus providing an independent check on the calculation that is based on the intensity of the fundamental. The displacement calculated from the ratio of the intensity of the overtone to the fundamental is 1.5 ± 0.3. This value is in excellent agreement with the value of 1.6 calculated above by using only the fundamental intensities. The agreement indicates that even when the absorption spectrum is broad and featureless, reliable displacements can be calculated from the combination of preresonance Raman data and electronic spectroscopy.

These data shed light on the underlying mechanism giving rise to the overtone intensity. Of the two possible limiting mechanisms derived from time-dependent theory, displaced excited states or vibrational frequency changes in excited states, the former is primarily responsible for the observed overtone intensity. If the overtone intensity were caused by a changed vibrational frequency in the excited state, a change of greater than 80% would be required in order to account for the measured intensity. Our data are in accord with the conclusion of Ziegler and Albrecht,[14] who considered seven origins of overtone intensity and found that the displaced excited-state mechanism is the most important as resonance is approached.

Summary

The time-dependent theory of molecular spectroscopy provides a reliable method of calculating electronic spectra from Raman spectroscopic data and of calculating the displacement of an excited-state potential surface along normal vibrational modes. A detailed test of the theory is provided by $Ph_2PS_2N_3$, where vibronic structure is found. For $Ph_4P_2S_2N_4$, where only a featureless electronic absorption band is observed, both the Raman fundamental intensities and the overtone intensity are used. In all cases, excellent agreement between theory and experiment is obtained.

Acknowledgment. The support of the U.S. Army Research Office and the National Science Foundation are gratefully acknowledged. We thank Prof. T. Chivers and Prof. W. G. Laidlow for the gift of the compounds and for helpful discussions.

Registry No. I, 76958-87-7; II, 85028-69-9.

---

[14] Ziegler, L. P.; Albrecht, A. C. *J. Raman Spectrosc.* **1979**, *8*, 73–80.